J. Am. Soc. Mass Spectrom. (2016) 27:646–661
DOI: 10.1007/s13361-016-1341-0

RESEARCH ARTICLE

Fragmentation Patterns and Mechanisms of Singly and Doubly Protonated Peptoids Studied by Collision Induced Dissociation

Jianhua Ren,[1] Yuan Tian,[1] Ekram Hossain,[1] Michael D. Connolly[2]

[1]Department of Chemistry, University of the Pacific, 3601 Pacific Avenue, Stockton, CA 95211, USA
[2]The Molecular Foundry, Lawrence Berkeley National Laboratory, Berkeley, CA 94720, USA

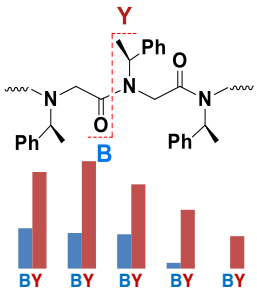

Abstract. Peptoids are peptide-mimicking oligomers consisting of N-alkylated glycine units. The fragmentation patterns for six singly and doubly protonated model peptoids were studied via collision-induced dissociation tandem mass spectrometry. The experiments were carried out on a triple quadrupole mass spectrometer with an electrospray ionization source. Both singly and doubly protonated peptoids were found to fragment mainly at the backbone amide bonds to produce peptoid B-type N-terminal fragment ions and Y-type C-terminal fragment ions. However, the relative abundances of B- versus Y-ions were significantly different. The singly protonated peptoids fragmented by producing highly abundant Y-ions and lesser abundant B-ions. The Y-ion formation mechanism was studied through calculating the energetics of truncated peptoid fragment ions using density functional theory and by controlled experiments. The results indicated that Y-ions were likely formed by transferring a proton from the C–H bond of the N-terminal fragments to the secondary amine of the C-terminal fragments. This proton transfer is energetically favored, and is in accord with the observation of abundant Y-ions. The calculations also indicated that doubly protonated peptoids would fragment at an amide bond close to the N-terminus to yield a high abundance of low-mass B-ions and high-mass Y-ions. The results of this study provide further understanding of the mechanisms of peptoid fragmentation and, therefore, are a valuable guide for de novo sequencing of peptoid libraries synthesized via combinatorial chemistry.

Keywords: Peptoid, N-alkylated glycine, CID, Fragmentation pattern, Protonated, Fragmentation mechanism, Y-ion formation mechanism

Received: 9 August 2015/Revised: 7 January 2016/Accepted: 9 January 2016/Published Online: 1 February 2016

Introduction

Peptoids are a class of peptidomimetic foldamers comprised of poly-*N*-alkylglycine [1–3]. Peptoids are bio-inspired polymers that are sequence-specific and that are able to fold into peptide-like secondary structures, and even into protein-like tertiary architectures [4–12]. Because of their diverse structures and tunable properties, peptoids have been an attractive molecular model for biophysical research. They have also been considered major candidates for peptide-mimicking therapeutic agents, ligands for proteins, and scaffolds in the search for new properties [3, 13–19]. Unlike peptides, peptoids are resistant to protease digestion, a property that results in high metabolic stability [20, 21]. Studies have shown that peptoids exhibit excellent biocompatibility in addition to biological activity [22, 23]. In recent years, peptoids have been successfully developed as antimicrobial agents, enzyme inhibitors, anti-fouling materials, antibody-mimetic materials, and biological antifreeze [12, 24–27]. Most of these studies relied on the creation of diverse peptoid libraries [28–30]. The discovery of these diverse and potentially useful properties of peptoid oligomers call for the development of efficient analytical methods to characterize the sequence and the structures of materials in these peptoid libraries just as in peptide libraries.

Conventional Edman degradation has been a common practice for direct sequencing of peptoids attached to solid resin supports. However, this method is extremely time-consuming as it requires the synthesis and analysis of standards for each residue [31–33]. Tandem mass spectrometry (MS/MS) techniques coupled with either electrospray ionization (ESI) or

Electronic supplementary material The online version of this article (doi:10.1007/s13361-016-1341-0) contains supplementary material, which is available to authorized users.

Correspondence to: Jianhua Ren; *e-mail:* jren@pacific.edu

matrix-assisted laser desorption/ionization (MALDI) are now routinely used for peptide and protein sequencing [34–37]. These tandem mass spectrometry based techniques have also shown promise as the method of choice for peptoid sequencing [29, 38–46]. We have previously studied the fragmentation patterns of a group of protonated and alkali-metallated peptoids under collision-induced dissociation (CID) as well as under electron capture dissociation (ECD) conditions [47, 48]. We observed characteristic fragmentations by both methods. Under the ECD condition, the primary backbone fragmentation occurred at the N–C_α bonds to produce C-ions (N-terminal fragments) and $Z^\bullet$-ions (C-terminal fragments). While the C-ions were observed for all the doubly protonated peptoids, the $Z^\bullet$-ions were observed only for the peptoids with a basic residue located at a position other than the N-terminus. Under CID conditions, the peptoids fragmented primarily at the amide bonds to produce B-ions (N-terminal fragments) and Y-ions (C-terminal fragments). These results were obtained by MALDI ionization with a linear ion trap mass spectrometer. Interestingly, the CID spectra of protonated peptoids contained only Y-type ions and not B-type ions, while the metallated peptoids produced comparably abundant B- and Y-ions. However, the MALDI instrument had a "low-mass cut-off" that precluded the detection of low-mass ions in the CID experiments. As a result of the limited data, the Y-ion formation mechanism could not be firmly established.

In order to characterize the mechanisms of peptoid fragment ion formation, we carried out subsequent tandem mass spectrometry studies on a series of model peptoids using triple quadrupole mass spectrometers with ESI ion sources. In this paper, we report the study of the fragmentation patterns and mechanisms of a group of model peptoids ionized by ESI and fragmented under CID conditions. The structures and the corresponding names of the model peptoids are shown in Scheme 1. The peptoid number is assigned based on our peptoid library sequence. The backbone structure of the peptoids P5, P6, P1, P3, and P4 consists of poly-(S)-N-(1-phenylethyl)glycine (abbreviated as poly-Nspe). Nspe has a chiral side-chain group and the structure of poly-Nspe is expected to be relatively rigid. Basic residues were attached at specific sites along the peptoid chain. The basic residues were either N-(2-aminoethyl)glycine (Nae) or N-(2-diisopropylaminoethyl)glycine (Ndipae). For the peptoid P10, the backbone consists of alternating N-(2-methoxyethyl)glycine (Nme) and N-(2-phenylethyl)glycine (Npe) residues. The achiral side-chain groups of these residues are less bulky, which allows conformational flexibility for the P10 oligomer. All our model peptoids are amidated at the C-terminus. P4 and P10 have a free amino N-terminus, and all other peptoids are acetylated at the N-terminus. These model peptoids readily form singly and doubly protonated ions under ESI conditions. These peptoids are designed to study the influence of charge location and charge state on the fragmentation patterns of the peptoid polymers in the gas-phase. The goal is to provide information leading to an understanding of the mechanisms of fragmentation so that rules for interpretation of spectra may be developed to do de novo sequencing of compounds such as those in peptoid libraries.

Experimental

Nomenclature of Peptoid Fragment Ions

Peptoids fragment in a manner similar to that of peptides under CID conditions [41, 42, 44, 47]. The main fragment ions observed correspond to the dissociation of the amide bonds of the peptoid backbone, which produce B- and Y-series ions (following the Roepstorff and Fohlman nomenclature[49]). In this paper, we applied similar nomenclature to characterize the fragment ions. However, we use capital letters, B or Y, to refer to peptoid ions instead of lower case letters, b or y, which are used for peptide ions. This capital letter convention was also used to refer to peptoid fragment ions by Liskamp and coworkers in their early publications [43, 44]. The fragmentation scheme and sample structures are shown in Scheme 2. The entries in Scheme 2 are only generic structures to illustrate as clearly as possible the fragmentation sites, the formal charges and to represent fragment ions. The actual structures, especially for the B-ions, are likely to be different from the generic species shown.

Mass Spectrometry Measurements

The mass spectrometry experiments were performed on two mass spectrometers: a Varian triple quadrupole mass spectrometer with an electrospray ionization (ESI) ion source (Varian 320 L; Varian Inc., now Agilent Technologies, Santa Clara, CA, USA), and a Thermo ESI-triple quadrupole mass spectrometer (TSQ Quantum; Thermo Scientific, San Jose, CA, USA). The peptoid sample solutions were prepared by dissolving 1 mg of solid peptoid into 1 mL of mixed solvent of water:methanol (1:1 v:v), and further diluted in the mixed solvent to a final concentration of ~10 μM. The sample solution was introduced into the ESI source by an infusion pump at a flow rate of 10 L/min (for the 320 L) or by injecting 20 μL of sample solution via a six-port valve into the LC flow (water:methanol 1:1) at 50 μL/min (for the TSQ Quantum). Both singly protonated and doubly protonated peptoid ions were readily generated by ESI. The monoisotopic peptoid ions were isolated for collision-induced dissociation (CID) experiments. To assign the type of the fragment ions, the *m/z* values of the monoisotopic peaks of all A-, B-, C-, X-, Y-, and Z-type ions of the model peptoids were calculated based on elemental compositions using ChemDraw (Chem&Bio Office, CambridgeSoft, now part of PerkinElmer Inc., Waltham, MA, USA). In addition, the *m/z* values were calculated to account for the observed losses of H_2O, NH_3, and other neutral molecules from the peptoid monomer side-chain groups.

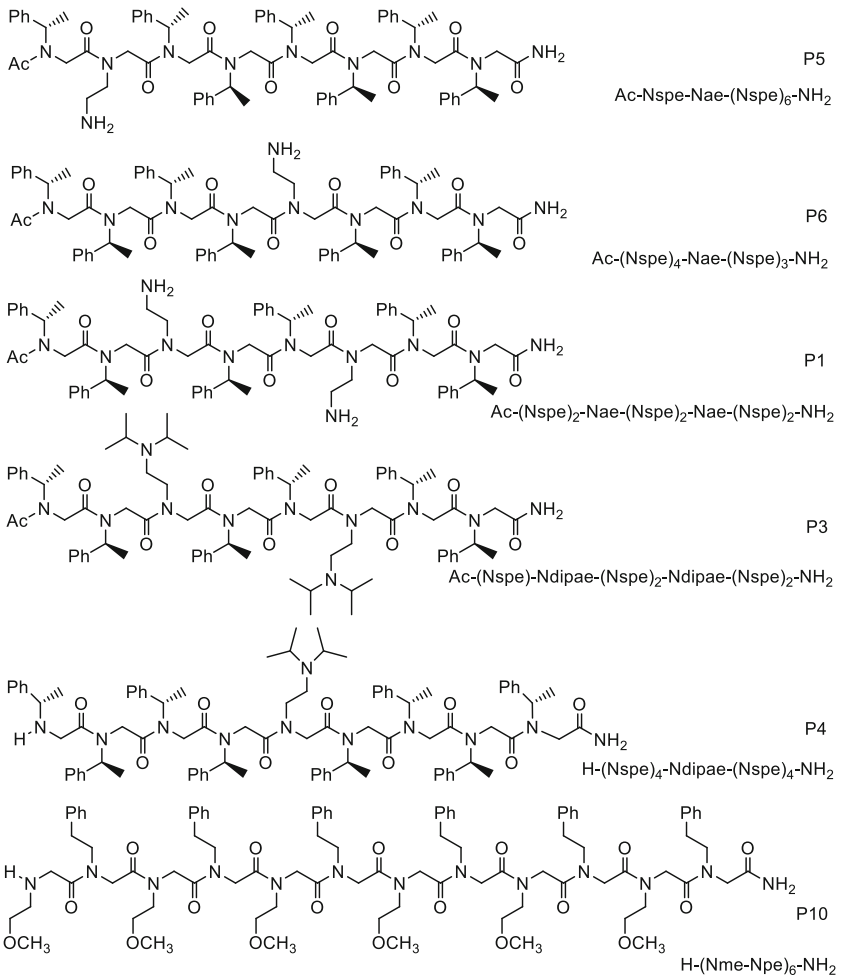

Scheme 1. Peptoid structures

The experimental conditions for the tandem mass spectrometry experiments are listed below. For the Varian 320 L instrument, the ESI needle voltage was 5 kV, capillary voltage 25 V, nebulizing gas (nitrogen) 50 psi, drying gas (nitrogen) temperature and pressure 200 °C and 18 psi, respectively, collision gas (argon) pressure 1.5 mTorr, collision energy ~45–50 eV for singly charged peptoids and ~10–15 eV for doubly charged peptoids, and data acquisition ~1–2 min. For the Thermo TSQ instrument, comparable standard ESI source parameters were used, including collision gas (argon) pressure 1.5 mTorr and collision energy ~40–47WalthameV for singly charged peptoids and ~12–15 eV for doubly charged peptoids.

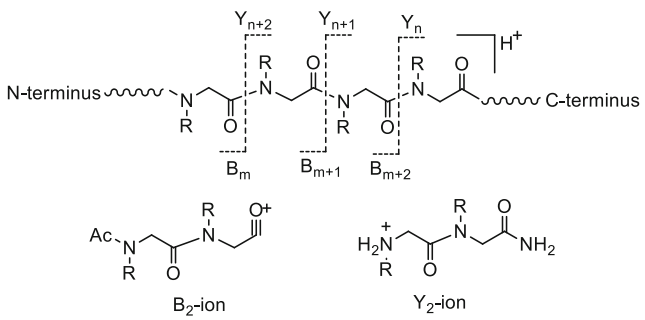

Scheme 2. Peptoid fragmentation ion nomenclature

Computational Method

The structures and energetics of the peptoid species were calculated at the B3LYP/6-31+G(d,p) level of theory. All computations were performed using the Gaussian 09 suite of programs [50]. The geometry optimization was followed by a frequency calculation to locate global minima and to yield unscaled zero-point energies and thermal corrections to 298 K. No imaginary frequency was observed for each structure, indicating that each had reached the energy minimum. The resulting electronic and thermal enthalpies, including zero-point correction, were used to calculate reaction enthalpies.

Peptoid Synthesis

All peptoids shown in Scheme 1 were synthesized using the solid-phase protocol with Rink amide resin (EMD Chemicals, Gibbstown, NJ, USA). The products were purified by HPLC and then freeze dried. A detailed synthesis procedure is described in our previous publication [47]. The four pentapeptoids with deuterium labeling were synthesized manually using a similar approach. The synthesis involved a two-step reaction cycle, bromoacetylation with bromoacetic acid followed by displacement of the bromine group with an amine

monomer. Deuterium labeling was achieved by using bromoacetic acid-d3 in the corresponding bromoacetylation step. The peptoid synthesis was performed at the Molecular Foundry at the Lawrence Berkeley National Laboratory.

Results

Peptoids 5, 6, and 1

P5, P6, and P1 are Nspe-based peptoids. P5 and P6 are isomers with one basic Nae residue inserted near the N-terminus and in the middle of the peptoid chain, respectively. P1 has two Nae residues. The CID spectra for the three peptoids recorded using the TSQ Quantum are shown in Figures 1 and 2. The spectra recorded using the Varian 320 L are shown in the supplementary material (Supplementary Figures S1, S2, and S3). All spectra are shown in relative abundances with the most abundant ion in each spectrum corresponding to 100% ion intensity. The singly protonated P5, *m/z* 1288 (Figure 1a), produced a high-abundance of Y-ions from Y_2 to Y_7, and a low-abundance of B-ions from B_1 to B_5. The ion at *m/z* 105 corresponded to a side-chain fragment ion, $[C_6H_5CHCH_3]^+$. The high mass ion at *m/z* 1184 corresponded to the loss of the side-chain group, $C_6H_5CH = CH_2$ (104 mass units), from $[P5 + H]^+$. The loss of 104 mass units was also observed for medium- to high-mass Y-ions. A notable ion at *m/z* 1270 about 18 mass units lower than the protonated P5 was found to be two peaks (Figure 1a insert), one corresponding to the loss of a water molecule (18 mass units) and the other to the loss of an ammonia molecule (17 mass units). The CID spectrum of the doubly protonated peptoid appeared dramatically different from that of the singly protonated one. Fragmentation of $[P5 + 2H]^{2+}$ *m/z* 644 (Figure 2a) produced the Y-series of ions, from Y_1 to Y_7, but all in relatively low abundance. Five B-ions, B_1 to B_5, were observed with the B_1-ion much more abundant than the other B-ions. The high abundance ion at *m/z* 105 was the side-chain fragment ion, $[C_6H_5CHCH_3]^+$. The ions at *m/z* 1184 and *m/z* 592 correspond to the loss of the neutral side-chain group of 104 mass units from the singly protonated and doubly protonated peptoid [(1185–104)/2 = 592], respectively.

The general fragmentation pattern of the singly protonated P6 was similar to that of P5, but the relative ion abundances were different. Fragmentation of $[P6 + H]^+$ (Figure 1b) produced the Y-series ions from Y_2 to Y_7 and two low abundant B-ions, B_1 and B_2. The side-chain fragment ion at *m/z* 105 was also observed. The loss of a neutral side-chain group of 104 mass units was observed for the peptoid ion and for high-mass Y-ions. The three Y-ions, Y_5 to Y_7, were accompanied by a pair of lower mass ions corresponding to the loss of water and ammonia, as indicated in the insert spectrum. The loss of ammonia, but not water, was observed for Y_4. The CID spectrum of the doubly protonated P6 (Figure 2b) showed relatively few fragment ions. The most abundant ions were B_1 and Y_7, followed by the side-chain fragment at *m/z* 105. The other ions were in low relative abundance.

Fragmentation of the singly protonated P1 *m/z* 1227 (Figure 1c) produced a high abundance of Y-ions from Y_2 to Y_7 and a relatively low abundance of B-ions from B_1 to B_3. The higher mass Y-ions (Y_4 to Y_7) as well as the peptoid precursor ion were accompanied by lower mass ions corresponding to the loss of a water molecule. The other notable ions included the side-chain fragment at *m/z* 105, and the loss of the side-chain group (104 mass units) from the peptoid ion, as well as Y_7 and B_2. The CID spectrum of the doubly protonated P1 *m/z* 614 (Figure 2c) appeared simple with a high abundance of ions for B_1, Y_7, and the side-chain fragment at *m/z* 105. The other observed fragment ions (B_2, and Y_2 to Y_6) were at low abundance. Ions corresponding to the loss of the side-chain group were also present in the spectrum. In particular, the doubly charged ion at *m/z* 562 corresponded to the loss of 104 mass units from the doubly protonated P1.

Peptoids 3 and 4

P3 is an analogue of P1 where there are two basic side-chain residues and both are Ndipae, which provide a bulky side-chain amino group (Scheme 1). P4 is an analogue of P6 where the basic side-chain group, Ndipae, is placed in the middle of the chain. P4 also differs from P6 in having a free amino N-terminus. Both P3 and P4 were difficult to fragment and required higher collision energy. CID spectra for P3 and P4 are shown in the supplemental material (Supplementary Figures S4 and S5), and their fragmentation schemes are shown in Figure 3. Fragmentation of $[P3 + H]^+$ *m/z* 1395 (Figure 3a and Supplementary Figure S4a) produced five Y-ions, Y_3 to Y_7, and four B-ions, B_1 to B_4. The Y-ions had much higher abundance than the B-ions. The side-chain fragment $[C_6H_5CHCH_3]^+$ at *m/z* 105 was present as well. The two peaks at *m/z* 1291 and *m/z* 1294 corresponded to the loss of the side-chain groups, $\mathbf{C}_6H_5CH = CH_2$ (104 mass units) and $(CH_3)_2CH\text{-}NH\text{-}CH(CH_3)_2$ (101 mass units), from $[P3 + H]^+$, respectively. Notice that water loss was not observed. Fragmentation of $[P3 + 2H]^{2+}$ *m/z* 698 (Supplementary Figure S4b) produced four observable Y-ions, Y_4 to Y_7, and two observable B-ions, B_1 and B_2. The intensities of B_1 and Y_7 were much greater than the other ions.

The fragmentation pattern of $[P4 + H]^+$ *m/z* 1491 (Figure 3b and Supplementary Figure S5a) looked similar to that of $[P3 + H]^+$ where a series of Y-ions, Y_3 to Y_8, were observed but only one B-ion, B_2, which was of low abundance. Notice that B_1 was not observed. The other notable ions were the side-chain fragment at *m/z* 105 and the loss of the side-chain group from the peptoid ion. For $[P_4 + 2H]^{2+}$ *m/z* 746 (Supplementary Figure S5b), the high abundance of ion was the side-chain fragment at *m/z* 105. The other notable ions were B_2, the loss of the side-chain group from B_2, and Y_5 to Y_7.

Peptoid 10

P10 consists of 12 monomer residues with alternating Nme and Npe groups and no basic side-chain groups. The N-terminus is a free secondary amine without acetylation. The CID spectra of

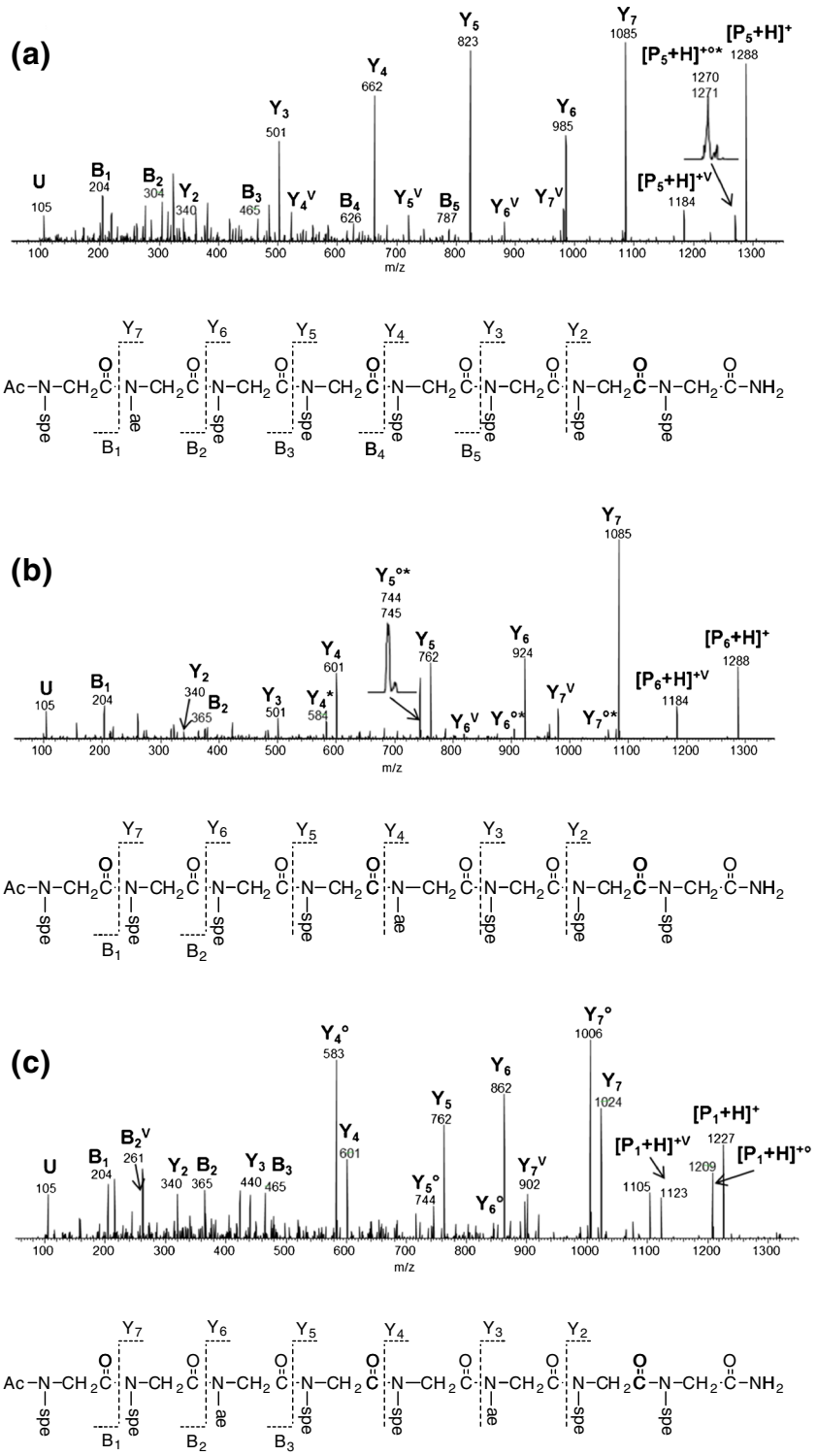

Figure 1. CID spectra of singly protonated peptoids, (**a**) $[P5 + H]^+$, (**b**) $[P6 + H]^+$, and (**c**) $[P1 + H]^+$, where U = $C_6H_5CHCH_3^+$, ^{V} represents the neutral loss of C_6H_5-CH = CH_2, * represents ammonia loss, and ° represents water loss

P10 are shown in Supplementary Figure S6, and the fragmentation scheme is shown in Figure 3. A higher collision energy was needed to fragment $[P10 + H]^+$ *m/z* 1675 (Figure 3c and Supplementary Figure S6a) and, even so, the intensities of the fragment ions were lower than 30% of that of the precursor peptoid ion. A series of B- and Y-ions from B_2 to B_8 and from Y_3 to Y_{11} were shown in the spectrum. Notice that B_1 was not observed. Fragmentation of $[P10 + 2H]^{2+}$ *m/z* 838 (Supplementary Figure S6b) produced two sets of ions, from B_2 to B_{10} and from Y_2 to Y_9.

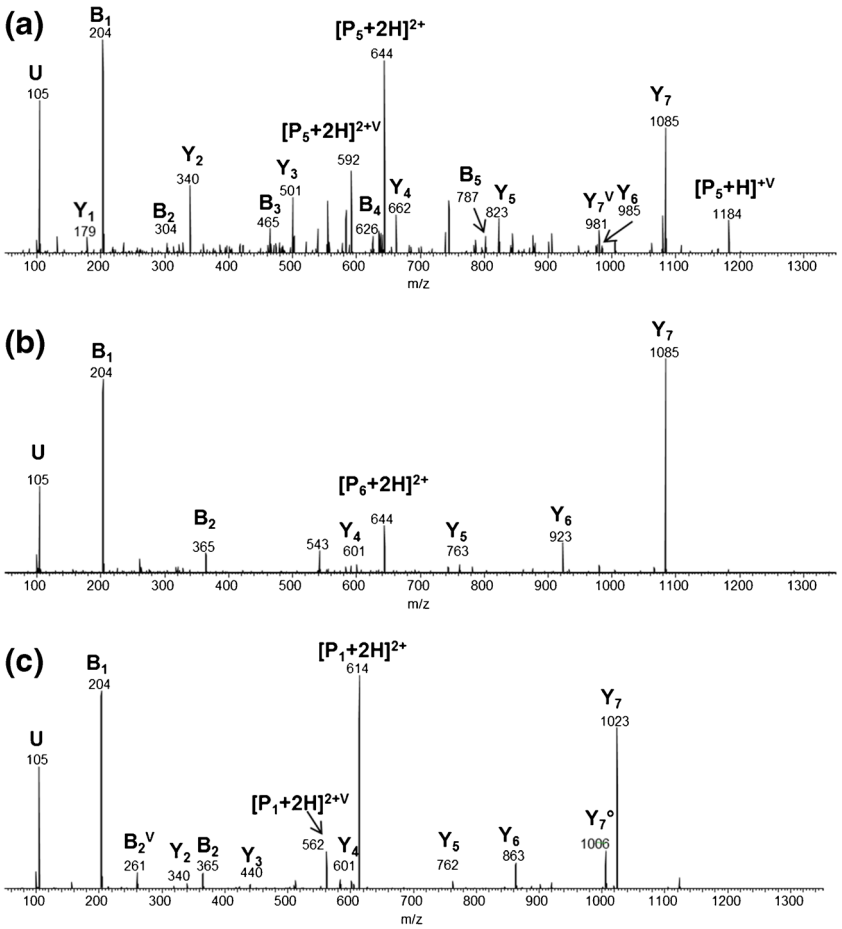

Figure 2. CID spectra of doubly protonated peptoids, (**a**) $[P5 + 2H]^{2+}$, (**b**) $[P6 + 2H]^{2+}$, and (**c**) $[P1 + 2H]^{2+}$, where U = $C_6H_5CHCH_3^+$, ^{V} represents the neutral loss of C_6H_5-CH = CH_2, and ° represents water loss

Peptoids 71–74

In order to help understanding peptoid fragmentation mechanisms, four deuterium labeled penta-peptoids were synthesized and their fragmentation patterns were examined. The structures of the peptoids are shown in Scheme 3 and their CID spectra are shown in Supplementary Figure S7. The truncated CID spectra for P72 and P74 along with key fragment ion structures are shown in Figure 4. The four peptoids consist of essentially the same sequence with alternating Nme and Npe residues. P71 and P73 have a free N-terminus, and P72 and P74 are acetylated at the N-terminus. Deuteration, replacing the backbone CH_2 with CD_2, occurs at the N-terminal residue for P71 and P72, and at the second residue from the N-terminus for P73 and P74. The fragmentation patterns for P72 and P74 appear similar with Y4 as the most abundant ion (Supplementary Figure S7). The *m/z* values suggest that Y4 of P72 and Y3 of P74 have acquired one deuterium atom, indicating that a deuterium has transferred from the CD_2 group to the C-fragment upon

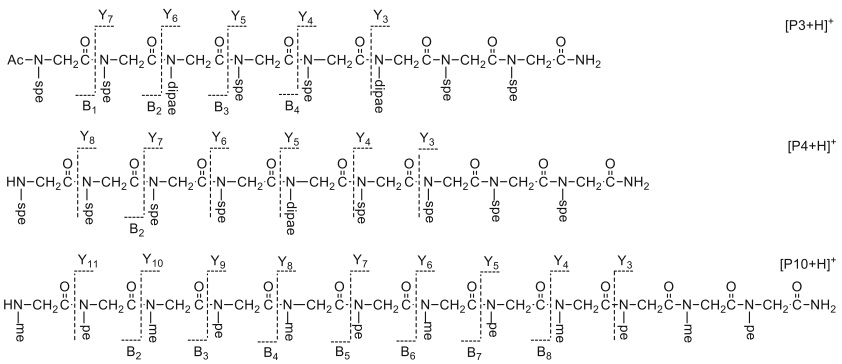

Figure 3. CID fragmentation schemes of singly protonated peptoids, $[P3 + H]^+$, $[P4 + H]^+$, and $[P10 + H]^+$

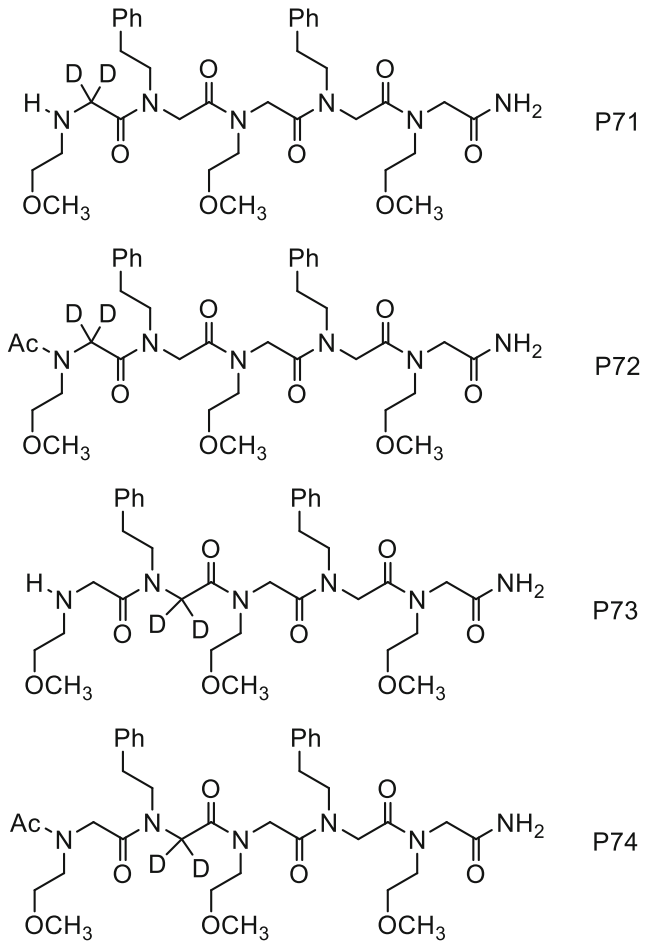

Scheme 3. Peptoid structures for P71–P74

dissociation at the adjacent amide bond (Figure 4a). The fragmentation patterns for P71 and P73 are also similar (Supplementary Figure S7). The Y4 ion of P71 and the Y3 ion of 73 were formed by abstracting a deuterium from the CD_2 group (Figure 4b).

Computational Results

In order to understand the possible mechanism of Y-ion formation, we calculated the enthalpy changes of proton transfer reactions between truncated N- and C-fragments. As shown in Scheme 4 and Supplementary Scheme S1), the reactions correspond to transferring a proton from an oxazolone B_2-ion to a C-terminal fragment to form the Y_3-ion. Three different monomer structures were selected, including N-methylglycine (R = CH_3), Nme (R = $CH_2CH_2OCH_3$), and Nspe (R = $CH_3CHC_6H_5$). The geometries and frequencies for all fragments were calculated at the B3LYP/6-31+G(d,p) level of theory. Selected optimized structures are shown in Supplementary Figure S8. The enthalpy changes for the proton transfer reactions are presented in Scheme 4 and Supplementary Scheme S1. Abstraction of the proton H_b from the backbone C–H bond did not change the oxazolone structure (Scheme 4A). The enthalpy change for the reaction was −3.0 kcal/mol (−12.5 kJ/mol) for R = CH_3, −5.4 kcal/mol (−22.6 kJ/mol) for R = $CH_2CH_2OCH_3$, and −0.5 kcal/mol (−2.1 kJ/mol) for R = $CH_3CHC_6H_5$. Abstraction of the proton H_c from the C–H bond in the oxazolone ring resulted in ring opening and formed a ketene structure (Scheme 4B). The overall enthalpy change for the proton transfer reaction was −2.0 kcal/mol (−8.4 kJ/mol) for R = CH_3, −1.0 kcal/mol (−4.2 kJ/mol) for R =

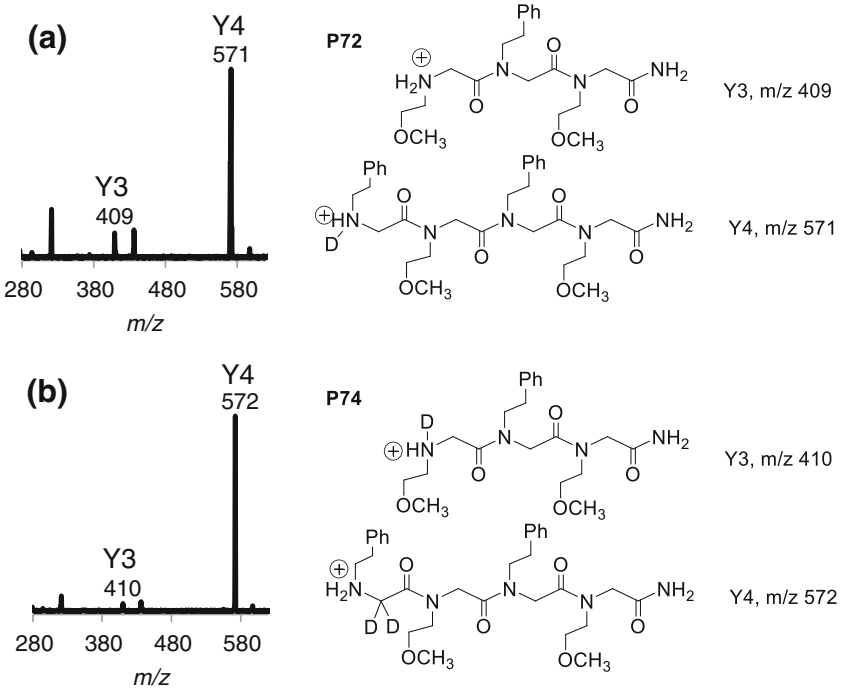

Figure 4. Truncated CID spectra for P72 and P74 along with structures of key fragment ions

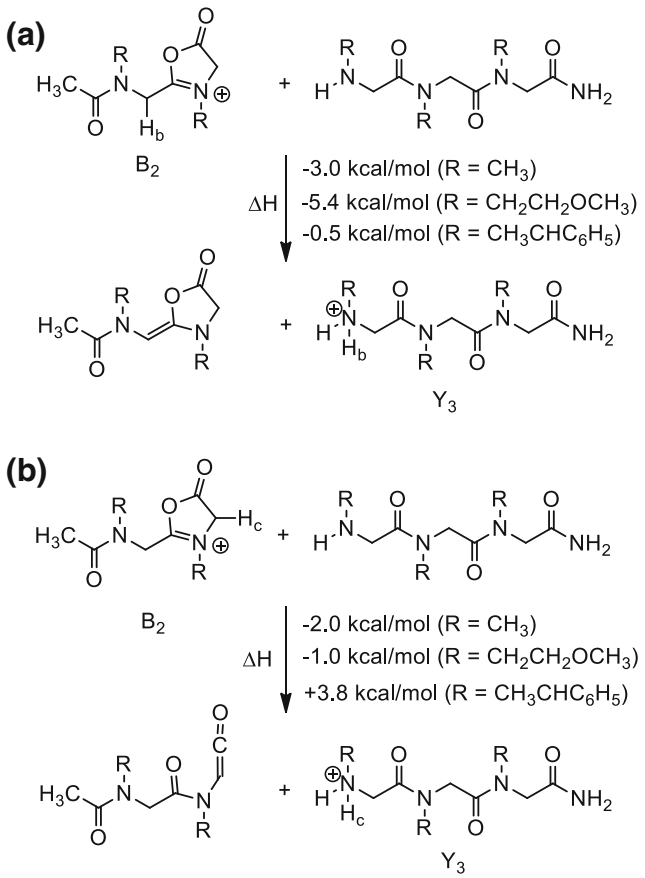

Scheme 4. Reaction enthalpies

$CH_2CH_2OCH_3$, and +3.8 kcal/mol (+15.9 kJ/mol) for R = $CH_3CHC_6H_5$. Abstraction of a proton from the side-chain C–H bond (bonded to the oxazolone nitrogen) gave an "ylide" structure at the N-fragment. The enthalpy changes for the proton transfer reactions with three different monomer residues were +29.7, +24.2, and +26.2 kcal/mol (or 124.1, 101.2, and 109.5 kJ/mol) for R = CH_3, $CH_2CH_2OCH_3$, and $CH_3CHC_6H_5$, respectively (Supplementary Scheme S1).

Discussion

Summary of the Fragmentation Patterns

To aid the comparison and discussion, the observed fragmentations for all of the model peptoids are summarized in Tables 1 and 2, and the relative ion abundance charts for selected peptoids are shown in Figures 5 and 6. Fragmentation of the singly charged peptoids required much higher collision energies than those for the doubly charged peptoids. In general, the singly protonated peptoids produced more observable fragment ions and the relative intensities of most fragment ions tended to be comparable, whereas the doubly protonated peptoids tended to produce one or two predominately abundant ions and the rest ions were at much lower abundances. The primary fragmentations of all the peptoids appeared to occur at the amide bonds and that yielded the B- and the Y-type ions. Regardless of singly or doubly charged peptoids, the low-mass B-ions and the high-mass Y-ions were relatively more abundant than the other ions. Interestingly, the B_1-ion was observed for all peptoids, except P_4 and P_{10}. Water loss was a significant secondary fragment for P1. Water- and ammonia losses were observed for P6 as well. The formation of the side-chain fragment ion, $[C_6H_5CHCH_3]^+$ (*m/z* 105), and the loss of the side-chain group, $C_6H_5CH = CH_2$ (104 u), appeared to be characteristic for all Nspe based peptoids.

Fragmentation Characteristics of Singly Protonated Peptoids

One common feature of the singly protonated peptoids was that fragmentation favored the production of low-mass B-type ions and medium- to high-mass Y-type ions. As shown in Figure 5, the fragmentation mainly occurred from the N-terminal side to the middle of the peptoid chain. For example, formation of B_1 and Y_7 from the three protonated peptoids (P5, P6, and P1) corresponded to the cleavage at the first amide bond from the N-terminus. In general, Y-ions were much more abundant than B-ions. The favoring of Y-ions suggested that the charge carrier (the proton) preferred to reside on the C-terminal fragments instead of on the N-terminal fragments. This fragmentation pattern was also observed in our previous study of peptoid ions generated by MALDI and collisionally dissociated in a linear quadrupole ion trap.[47] That study showed that the protonated peptoids fragmented by producing predominantly Y-type ions and B-type ions were nearly completely absent in the CID spectra. The absence of the B-ions was probably due to the low mass cut-off in the ion trap and, consequently, the low-mass B-ions were not detected. The preference for the formation of Y-type ions has also been observed by other researchers [44]. The fragmentation patterns of protonated peptoids appeared quite different from those of most protonated peptides. For protonated peptides without terminal modifications and without basic side chains, the predominant fragments are often b-type ions. The preference for b-type ions has also been observed in peptides with N-terminal acetylation and C-terminal esterification [51]. For peptides with a basic residue (e.g., lysine or arginine), the major fragments have been shown to vary depending on the location of the basic residue [52].

The other common feature of the singly protonated peptoids is that the location of the basic Nae residue seems to have minimal influence on the overall fragmentation pattern (the relative abundances of the fragment ions). This was seen in the isomeric peptoids with the Nae residue located at different sites (Figure 5). In P5, the more abundant Y-ions (Y_3 to Y_6) did not contain the Nae residue. P6 had the Nae residue inserted in the middle of the peptoid chain, yet the most abundant Y-ion was the one from fragmentation at the N-terminal amide bond. While not influencing the fragmentation patterns, the Nae residue did enhance the fragmentation efficiency. All peptoids containing the Nae residue produced abundant fragment ions at a relatively lower collision energy (40 eV). The three peptoids

Table 1. Fragmentation Patterns for the Singly Protonated Peptoids,[a] $[P + H]^+$

Peptoid	B_1	B_2	B_3	B_4	B_5	B_6	B_7	B_8	B_9	Y_2	Y_3	Y_4	Y_5	Y_6	Y_7	Y_8	Y_9	Y_{10}	Y_{11}	$[P + H]^+$
P5	x	x	x	x	x					x	x	x^V	x^V	x^V	x^V					$*^{O V}$
P6	x	x								x	x	x*	x^{*O}	x^{*O}	x^{*O}					
P1	x	x^V	x							x	x	x^O	x^O	x^O	$x^{O V}$					$^{O V}$
P3	x	x	x	x							x	x	x	x	x					^{V}
P4		x									x	x	x	x	x	x				^{V}
P10		x	x	x	x	x	x	x			x	x	x	x	x	x	x	x	x	

[a] The symbol x indicates the observed ions with relative abundance of 3% or higher.
[O] Accompanied by the loss of water molecule.
* Accompanied by the loss of ammonia molecular.
[V] Accompanied by the loss of a side-chain group of 104 u.

without the Nae residue, P10 (without a basic side-chain group), P3 (with one Ndipae residue), and P4 (with two Ndipae residues), yielded relatively low abundance of fragment ions even at a higher collision energy (50 eV).

Fragmentation Mechanism: Y-Ion Formation

The observed bias towards Y-ion formation, the minimal influence of the Nae residue on fragmentation patterns, and the significant influence of the Nae residue on fragmentation efficiency could be explained by a mechanism considering (1) the "mobile proton," and (2) the relative basicity of the fragments. The original "mobile proton model" was proposed by Gaskell and Wysocki plus their coworkers to explain the fragmentation of protonated peptides. This model assumes that, upon collision, the proton(s) move(s) to various protonation sites and induce(s) fragmentations [53, 54]. This model has been successfully used to describe the fragmentation mechanisms of various protonated peptides [37].

Our proposed mechanism for the dissociation of the amide bonds to form peptoid B- and Y-ions is shown in Scheme 5 where the dashed circle indicates the "mobile proton." It is postulated that prior to collision with argon atoms, the charge carrier, the proton, resides at the most basic site of the peptoid, such as the side-chain amino group or the free amino group at the N-terminus. Upon collision, the proton migrates to various amide bonds and induces fragmentations. Scheme 5A illustrates that once the carbonyl group of the amide has acquired a proton, the group is activated and allows an intramolecular addition-elimination reaction to occur. A nearby amide oxygen 1atom serves as a nucleophile to attack the activated carbonyl group to form a five-membered ring intermediate. This leads to dissociation of the C–N bond to form an ion-neutral complex of an oxazolone ion at the N-fragment and a secondary amine at the C-fragment. Dissociation of this complex ion would yield a peptoid oxazolone B-ion and a neutral C-fragment. One remaining question is "how are the peptoid Y-ions formed?" Formation of a peptoid Y-ion would require a proton transfer from the charged N-fragment to the neutral C-fragment prior to or upon dissociation of the ion-neutral complex. The likely proton source is either the backbone C–H_b bond adjacent to the oxazolone ring (Scheme 5B), or the C–H_c bond in the oxazolone ring (Scheme 5C). Notice that in Scheme 5C, the neutral N-fragment is a ketene structure, which is suggested by computational results (Scheme 4B). The explanation is given in conjunction with a comparison to the mechanism of peptide fragmentation shown in Scheme 6.

The formation of oxazolone B-ions is supported by the fact that the B_1-ion was observed for all of the model peptoids with N-terminal acetylation, but not for the two peptoids, P4 and P10, without acetylation. Formation of the oxazolone B_1-ion would require the participation of the acetyl group such that the oxygen atom of the acetyl group serves as the nucleophile (Scheme S2). P4 and P10 do not have an acetyl group and the B_1-ion was not formed.

Scheme 6 shows the established mechanism (by other researchers) of peptide fragmentation, where the oxazolone pathway would yield both peptide b- and y-ions [37]. Upon

Table 2. Fragmentation Patterns for the Doubly Protonated Peptoids,[a] $[P + 2H]^{2+}$

Peptoid	B_1	B_2	B_3	B_4	B_5	B_6	B_7	B_8	B_9	B_{10}	Y_1	Y_2	Y_3	Y_4	Y_5	Y_6	Y_7	Y_8	Y_9	$[P + 2H]^{2+}$
P5	x	x	x	x	x						x	x	x	x	x	x^V	x^V			^{V}
P6	x	x												x	x	x	x			
P1	x	x^V										x	x	x	x	x	$x^{O V}$			^{V}
P3	x	x												x	x	x	x			
P4		x^V													x	x	x			
P10		x	x	x	x	x	x	x	x	x		x	x	x	x	x	x	x	x	

[a] The symbol x indicates the observed ions with relative abundance of 3% or higher.
[O] Accompanied by the loss of water molecule.
* Accompanied by the loss of ammonia molecular.
[V] Accompanied by the loss of a side-chain group of 104 u.

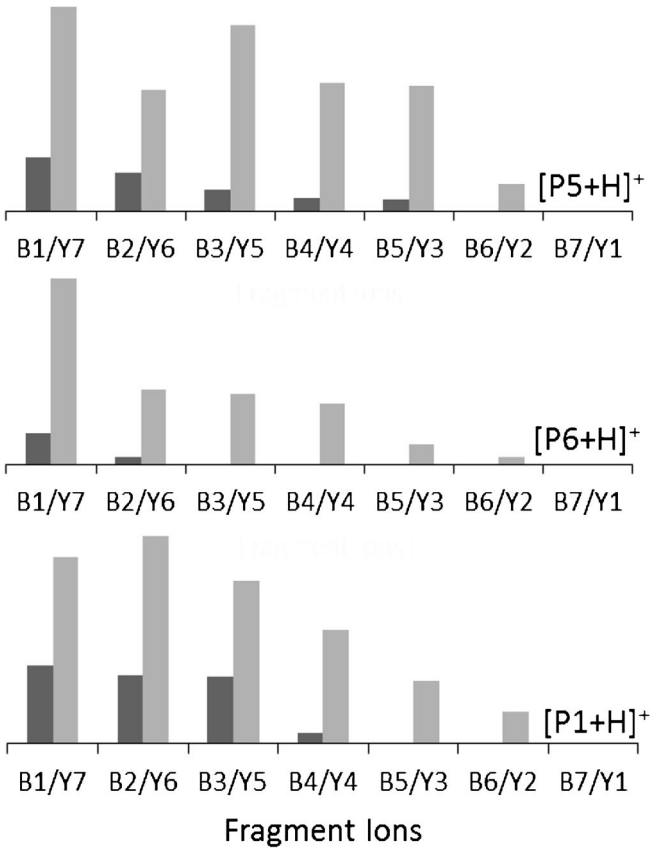

Figure 5. Relative abundance chart of B- and Y-ions resulting from singly protonated peptoids: P5, P6, and P1, where the darker bars represent the B-ions and the lighter bars are for the Y-ions

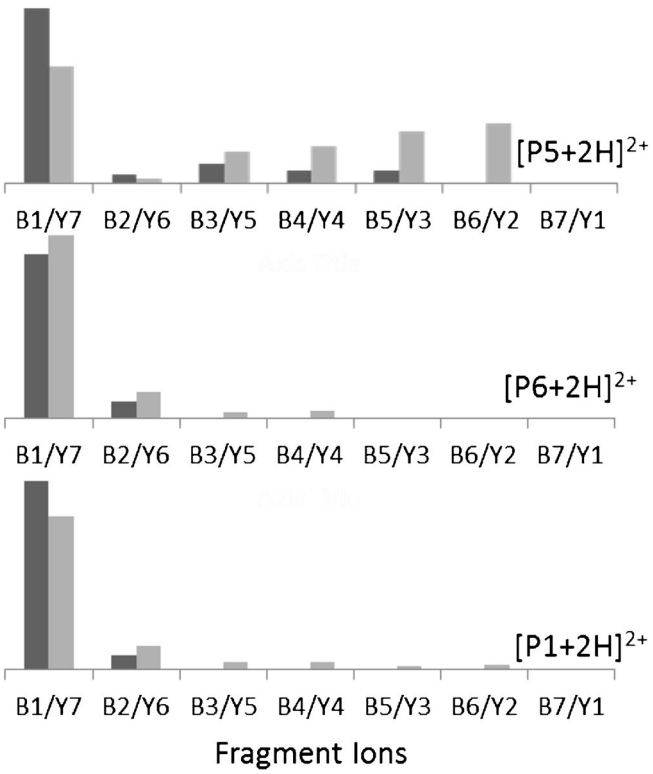

Figure 6. Relative abundance chart of B- and Y-ions resulting from doubly protonated peptoids: P5, P6, and P1, where the darker bars represent the B-ions and the lighter bars are for the Y-ions

activation of an amide bond by the mobile proton, an intramolecular addition-elimination leads to the dissociation of the amide bond to form an oxazolone ion as part of the N-fragment and a primary amine as part of the C-fragment. The ion and the neutral are held together as an ion-neutral complex. Direct dissociation of this ion-neutral complex yields a peptide b-ion and a neutral C-fragment. Notice that the oxazolone ring has a tertiary ammonium cation with an acidic N–H_a bond. If prior to or upon dissociation of the complex ion, the acidic hydrogen, H_a, transfers to the amino group of the C-fragment, a peptide y-ion would form. A control study by Paizs et al. using H-Gly-Sar-Sar-OH showed that when the peptide amide hydrogen atom (H_a) was replaced by a methyl group, the y-ion (y_1-ion in this case) formation was reduced dramatically [55]. This study suggested that the presence of the acidic N–H_a bond was crucial for the formation of peptide-y-ions. Recently, Szewczuk and coworkers carried out a series of studies on the fragmentation pathways in N-substituted oligopeptides, including oligoproline and oligosarcosine, with a quaternary ammonium (QA) group tagged at the N-terminus [56, 57]. These peptides did not contain backbone N–H groups. Their results showed that the fragmentation was initiated by eliminating the quaternary ammonium group, which generated a mobile proton. The mobile proton would induce a charge-directed fragmentation of an amide bond and this process was accompanied by shifting another proton from a C–H bond to the C-fragment. This resulted in a neutral ketene structure at the N-fragment and a y-type ion at the C-fragment. Their studies on deuterated QA-tagged oligosarcosine further showed that formation of y-ions involved the migration of a proton from the α-C–H bond of sarcosine residue [56].

For peptoids, the oxazolone B-ion is a quaternary ammonium cation. The acidic N–H_a bond is absent in the peptoid oxazolone and, therefore, the acidic proton has to come from a different site. The three potential sites of a proton donor are the backbone C–H bond adjacent to the oxazolone ring, the C–H group in the oxazolone ring, and the C–H bond of the side-chain group bound to the oxazolone nitrogen. Our calculations at the B3LYP/6-31+G(d,p) level of theory suggested that the enthalpy change for abstracting proton H_b from the backbone C–H bond is −3.0 kcal/mol (−12.5 kJ/mol) for R = CH_3, −5.4 kcal/mol (−22.6 kJ/mol) for R = $CH_2CH_2OCH_3$, and −0.5 kcal/mol (−2.1 kJ/mol) for R = $CH_3CHC_6H_5$ (Scheme 4A). This suggests that transferring a proton from the C–H bond to the amino group of the C-fragment is energetically favored. The calculation also showed that the enthalpy change for the abstraction of proton H_c from the C–H bond in the oxazolone ring is −2.0, −1.0, and +3.8 kcal/mol (or −8.4, −4.2, and +15.9 kJ/mol) for R = CH_3, $CH_2CH_2OCH_3$, and $CH_3CHC_6H_5$, respectively (Scheme 4B). The smaller negative to positive enthalpy change indicates that abstracting a proton from the oxazolone ring is less favorable than abstracting the

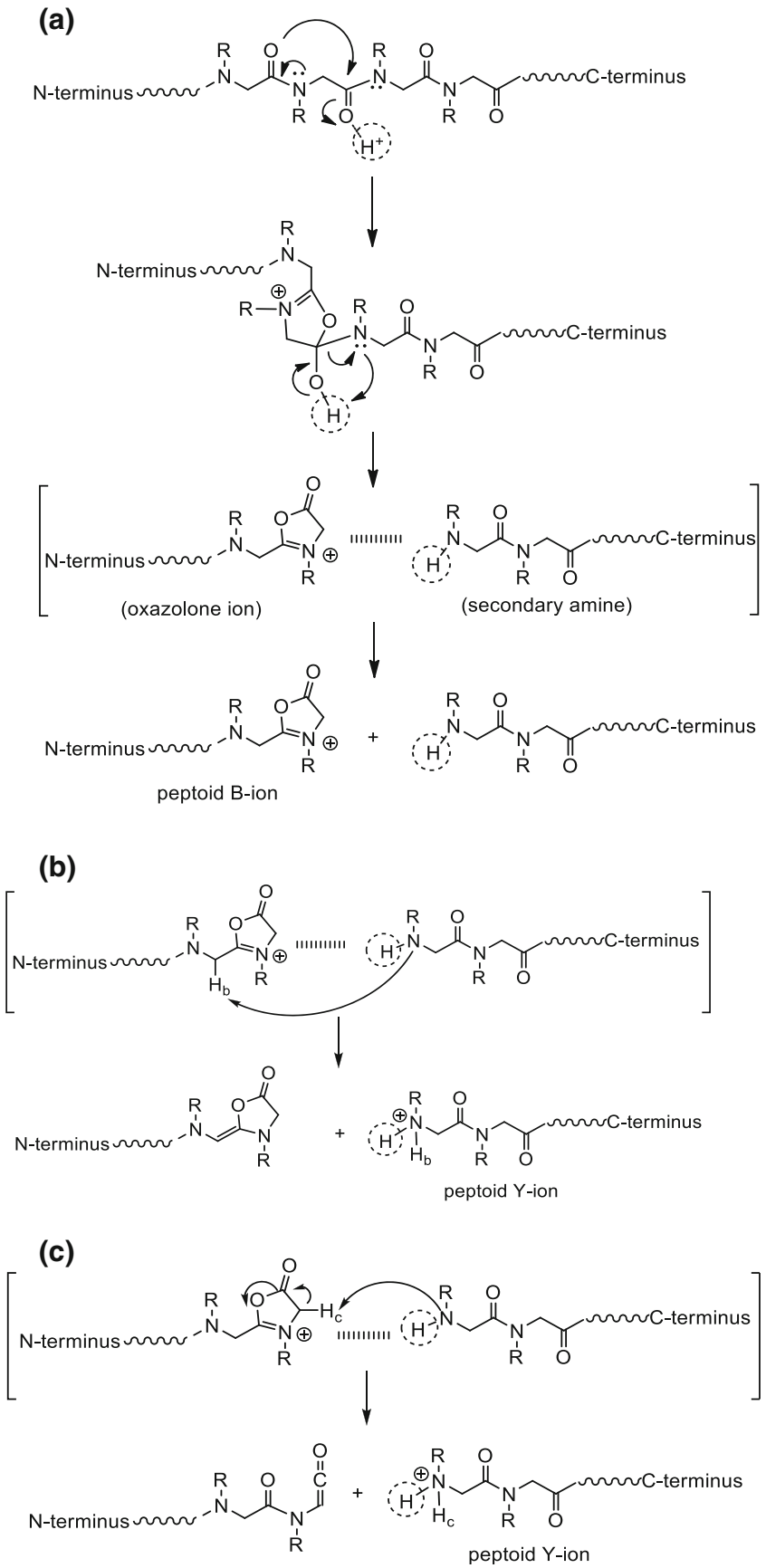

Scheme 5. Proposed peptoid fragmentation mechanism

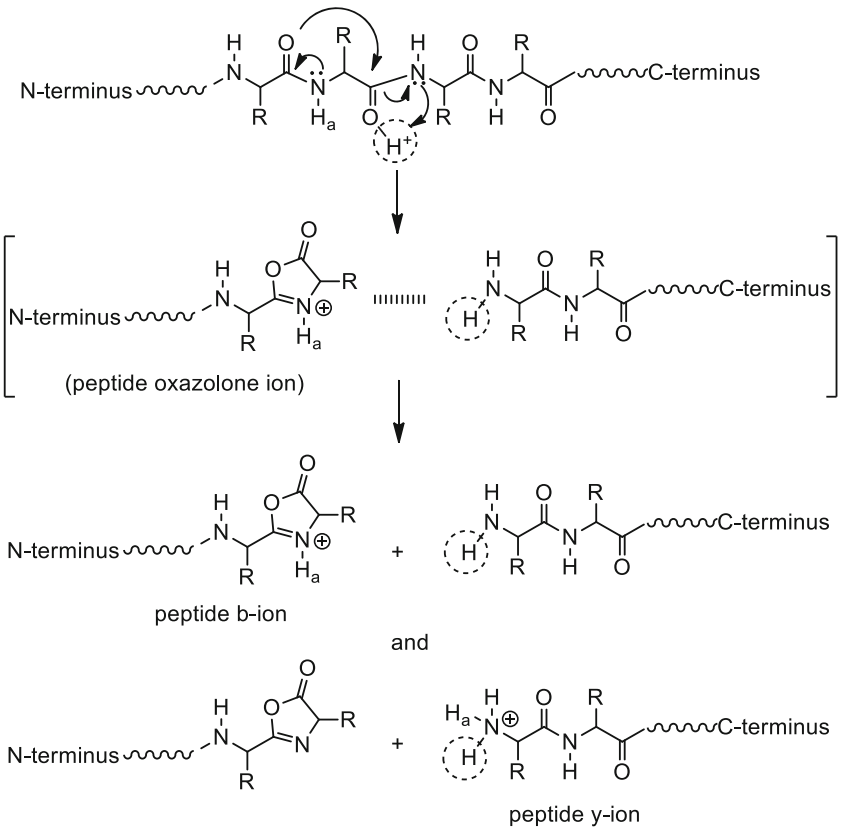

Scheme 6. Peptide fragmentation pathway

proton from the backbone C–H group, but is also likely considering that the proton transfer occurs within the ion-neutral complex and not between two isolated molecular species. Furthermore, our calculations indicated that the enthalpy change for abstracting a proton from the C–H bond of the side-chain group of oxazolone is largely positive (Scheme S1) and, therefore, the reaction is not likely to occur. Computational results suggested that formation of peptoid Y-ions is energetically favored over the formation of peptoid B-ions, and the Y-ion formation proceeds by the abstraction of a proton from a backbone C–H group of the N-fragment upon dissociation of the protonated amide bond. However, computational results cannot rule out either of the processes shown in Scheme 5B or C.

Control studies using deuterium labeled peptoids suggest that a Y-ion is formed by abstracting a proton from a C–H bond of the N-fragment adjacent to the dissociating amide bond, for example Y4 of P72 and Y3 of P74 (Figure 4). The acidic C–H group corresponds to the C–H_c bond in the oxazolone ring and, hence, the results from the control studies support the mechanism shown in Scheme 5C.

The computed enthalpy value indicates that the proton affinity of the C-fragment is higher than that of the N-fragment and, therefore, the charge-carrier proton preferentially resides at the C-fragments to form the peptoid Y-ions. In general, the proton affinity increases with the size of a molecule. The longer C-fragments would have higher proton affinities than the shorter ones. Longer C-fragments require fragmentation to occur at the amide bonds closer to the N-terminus. These predictions agree well with the observations that Y-ions were more abundant than B-ions, and medium- to high-mass Y-ions were more abundant than low-mass Y-ions, whereas low-mass B-ions were more favored than high-mass B-ions.

Our results also showed that the Nae residue had a small effect on the relative abundances of the fragment ions. Nae has a basic side-chain group, a primary amine, which is expected to be a protonation site. One would expect that the fragment ions containing a Nae residue would show high abundances. Yet the most abundant Y-ions did not contain a Nae residue. The minimal influence of the basic Nae residue on the fragmentation patterns could be explained based on the relative proton affinity of different amino groups. Upon fragmentation of a peptoid amide bond, a secondary amine is formed as part of the C-fragment (for peptides, fragmentation of an amide bond forms a primary amine as part of the C-fragment). The proton affinities for different types of amines follow the general trend: tertiary amine > secondary amine > primary amine > amide. A relevant example is the relative proton affinity between alanine (a primary amine) and sarcosine (N-methylamine, a secondary amine). The proton affinity for sarcosine is 220.2 kcal/mol (920.4 kJ/mol), which is about 5 kcal/mol (20 kJ/mol) higher than that for alanine (215.2 kcal/mol or 899.5 kJ/mol). A higher proton affinity indicates a higher possibility of acquiring a proton upon fragmentation. The side-chain of the Nae residue is a primary amine, whereas the C-terminal fragment is a secondary amine. The higher proton affinity of the secondary amine would compete for the proton more favorably than a primary amine.

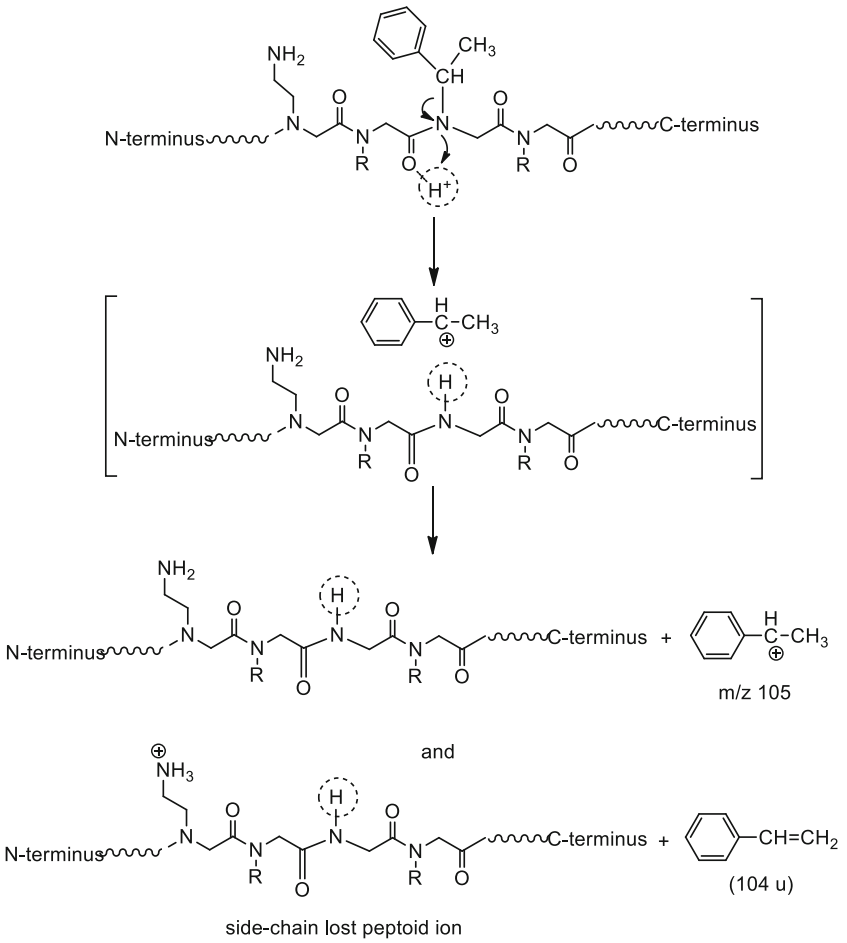

Scheme 7. Side-chain loss mechanism

Fragmentation Mechanism: the Side-Chain Loss

The loss of the side-chain group, $C_6H_5CH = CH_2$ (104 mass units), and the formation of the side-chain fragment ion at *m/z* 105, $[C_6H_5CHCH_3]^+$, were common for all Nspe-containing peptoids. The ion at *m/z* 105 was commonly observed and, in some cases, this ion was the base peak in the CID spectra. The mechanism for the loss of the side-chain from a peptoid ion and the formation of the side-chain fragment ion is shown in Scheme 7. Upon acquisition of the "mobile proton" by an

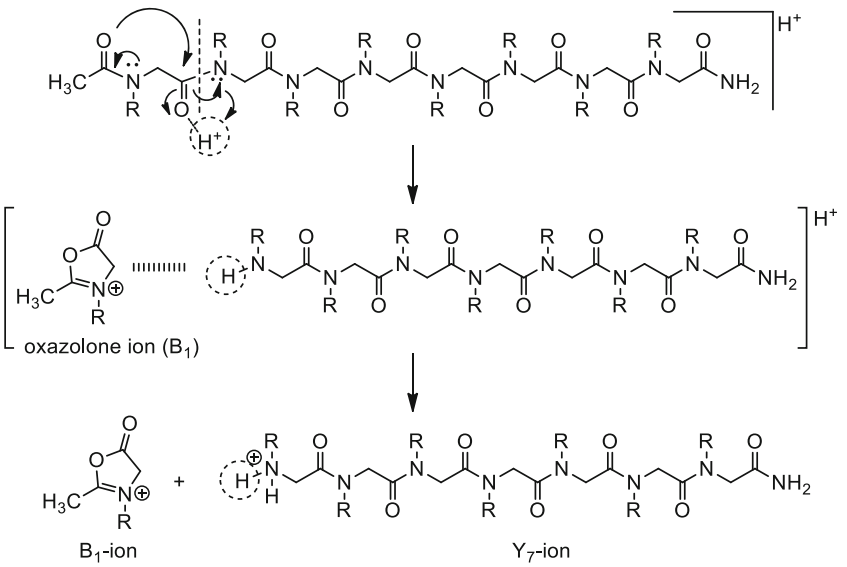

Scheme 8. Fragmentation scheme of doubly protonated peptoids

amide group of an Nspe residue, the N–C bond of the Nspe dissociates heterolytically to form a benzylic cation (*m/z* 105) and a neutral peptoid. If a proton from the benzylic cation is transferred to a basic site, such as the side-chain amino group of the Nae residue, a peptoid ion (missing the side chain) would form along with a neutral alkenyl benzene (104 mass units).

Fragmentation Characteristics and Mechanism of Doubly Protonated Peptoids

Unlike the singly protonated peptoids discussed above that fragment at various amide bonds and produce abundant Y-ions (Figure 5), the doubly protonated peptoids fragment primarily at the amide bond close to the N-terminus and yield primarily B_1- and Y_7-ions (Figure 6). The basic Nae residue seems to have minimal effect on the fragmentation pattern. A schematic mechanism for the formation of B_1 and Y_7 ions is shown in Scheme 8, where the vertical dashed line indicates the fragmentation site. Upon collisional activation, the two protons residing on the peptoid become mobile. One proton induces the dissociation of an amide bond close to the N-terminus as indicated by the vertical dashed line. This yields an oxazolone ion (B_1) as the N-fragment and a secondary amine as the C-fragment with the two fragments associated as a complex. Upon dissociation of the complex, the N-fragment remains as a B_1-ion, and the second proton would move to and be bound to the secondary amine of the C-fragment to form the Y_7-ion. Since the C-fragment does not need to abstract a proton from the N-fragment, as in the case of the singly protonated peptoids, both the B_1-ion and the Y_7-ion are observed in high abundance. Columbic repulsion between the two charges suggests that the mobility of the two protons would be limited. This might explain the paucity of fragment ions observed in doubly protonated peptoids. The preference to form low-mass B-ions might be due to minimal steric constraint, whereas the longer Y-ions might be due to higher net proton affinity.

Conclusions

The fragmentation patterns for six model peptoids were studied under collision-induced dissociation conditions. The main fragmentation sites were the backbone amide bonds and resulting fragments were B- and Y-ions. Both singly and doubly protonated peptoids were studied. The singly protonated peptoids fragmented by producing a high abundance of Y-ions and a low abundance of B-ions. The B-ions were likely formed via an oxazolone pathway. The Y-ions were formed by abstracting a proton from the backbone C–H bond adjacent to the dissociating amide bond. Computational studies suggested that transferring a proton from the N-fragment to the secondary amine of the C-terminal fragment was energetically favored and, therefore, supported the observed fragmentation bias toward Y-ions. The doubly protonated peptoids were observed to fragment at an amide bond close to the N-terminus and to yield primarily low-mass B-ions and high-mass Y-ions. This feature is likely due to the fact that formation of low-mass oxazolone B-ions is kinetically favored and formation of high-mass Y-ions is thermodynamically favored. The results from this study provide further understanding of the mechanisms of peptoid fragmentation. This insight, which is based on calculations and observed CID fragmentation of model peptoids, should be valuable in generating fragmentation rules for de novo peptoid sequencing of combinatory peptoids.

Acknowledgments

The authors thank Dr. David Robinson (Sandia National Laboratories) for providing peptoid samples, and Dr. Ronald Zuckermann (The Molecular Foundry, Lawrence Berkeley National Laboratory) for supporting the peptoid synthesis. All peptoids, including deuterium labeled peptoids, were synthesized at the Molecular Foundry. Work at the Molecular Foundry was supported by the Office of Science, Office of Basic Energy Sciences, of the U.S. Department of Energy under Contract no. DE-AC02-05CH11231. J.R. acknowledges the support from the National Science Foundation (CHE-1301505). The authors thank Dr. Patrick Jones (University of the Pacific) for proof-reading the manuscript. All mass spectrometry experiments were conducted at the Chemistry Mass Spectrometry Facility at the University of the Pacific.

References

1. Farmer, P.S., Ariens, E.J.: Speculations on the design of nonpeptidic peptidomimetics. Trends Pharmacol. Sci. **3**, 362–365 (1982)
2. Simon, R.J., Kania, R.S., Zuckermann, R.N., Huebner, V.D., Jewell, D.A., Banville, S., Ng, S., Wang, L., Rosenberg, S., Marlowe, C.K., Spellmeyer, D.C., Tan, R., Frankel, A.D., Santi, D.V., Cohen, F.E., Bartlett, P.A.: Peptoids: a modular approach to drug discovery. Proc. Natl. Acad. Sci. U. S. A. **89**, 9367–9371 (1992)
3. Sun, J., Zuckermann, R.N.: Peptoid polymers: a highly designable bioinspired material. ACS Nano **7**, 4715–4732 (2013)
4. Paul, B., Butterfoss, G.L., Boswell, M.G., Renfrew, P.D., Yeung, F.G., Shah, N.H., Wolf, C., Bonneau, R., Kirshenbaum, K.: Peptoid atropisomers. J. Am. Chem. Soc. **133**, 10910–10919 (2011)
5. Burkoth, T.S., Beausoleil, E., Kaur, S., Tang, D., Cohen, F.E., Zuckermann, R.N.: Toward the synthesis of artificial proteins. The discovery of an amphiphilic helical peptoid assembly. Chem. Biol. **9**, 647–654 (2002)
6. Kirshenbaum, K., Barron, A.E., Goldsmith, R.A., Armand, P., Bradley, E.K., Truong, K.T.V., Dill, K.A., Cohen, F.E., Zuckermann, R.N.: Sequence-specific polypeptoids: a diverse family of heteropolymers with stable secondary structure. Proc. Natl. Acad. Sci. U. S. A. **95**, 4303–4308 (1998)
7. Wu, C.W., Sanborn, T.J., Huang, K., Zuckermann, R.N., Barron, A.E.: Peptoid oligomers with alpha-chiral, aromatic side chains: sequence requirements for the formation of stable peptoid helices. J. Am. Chem. Soc. **123**, 6778–6784 (2001)
8. Wu, C.W., Sanborn, T.J., Zuckermann, R.N., Barron, A.E.: Peptoid oligomers with alpha -chiral, aromatic side chains: effects of chain length on secondary structure. J. Am. Chem. Soc. **123**, 2958–2963 (2001)
9. Wu, C.W., Kirshenbaum, K., Sanborn, T.J., Patch, J.A., Huang, K., Dill, K.A., Zuckermann, R.N., Barron, A.E.: Structural and spectroscopic studies of peptoid oligomers with alpha-chiral aliphatic side chains. J. Am. Chem. Soc. **125**, 13525–13530 (2003)

10. Lee, B.-C., Zuckermann, R.N., Dill, K.A.: Folding a nonbiological polymer into a compact multihelical structure. J. Am. Chem. Soc. **127**, 10999–11009 (2005)
11. Lee, B.-C., Chu, T.K., Dill, K.A., Zuckermann, R.N.: Biomimetic nanostructures: creating a high-affinity zinc-binding site in a folded nonbiological polymer. J. Am. Chem. Soc. **130**, 8847–8855 (2008)
12. Olivier, G.K., Cho, A., Sanii, B., Connolly, M.D., Tran, H., Zuckermann, R.N.: Antibody-mimetic peptoid nanosheets for molecular recognition. ACS Nano **7**, 9276–9286 (2013)
13. Nguyen, J.T., Turck, C.W., Cohen, F.E., Zuckermann, R.N., Lim, W.A.: Exploiting the basis of proline recognition by SH3 and WW domains: design of N-substituted inhibitors. Science **282**, 2088–2092 (1998)
14. Chongsiriwatana, N.P., Patch, J.A., Czyzewski, A.M., Dohm, M.T., Ivankin, A., Gidalevitz, D., Zuckermann, R.N., Barron, A.E.: Peptoids that mimic the structure, function, and mechanism of helical antimicrobial peptides. Proc. Natl. Acad. Sci. U. S. A. **105**, 2794–2799 (2008)
15. Kruijtzer, J.A.W., Nijenhuis, W.A.J., Wanders, N., Gispen, W.H., Liskamp, R.M.J., Adan, R.A.H.: Peptoid–peptide hybrids as potent novel melanocortin receptor ligands. J. Med. Chem. **48**, 4224–4230 (2005)
16. Liu, B., Alluri, P.G., Yu, P., Kodadek, T.: A potent transactivation domain mimic with activity in living cells. J. Am. Chem. Soc. **127**, 8254–8255 (2005)
17. Patch, J.A., Barron, A.E.: Helical peptoid mimics of magainin-2 amide. J. Am. Chem. Soc. **125**, 12092–12093 (2003)
18. Ruijtenbeek, R., Kruijtzer, J.A.W., Van de Wiel, W., Fischer, M.J.E., Fluck, M., Redegeld, F.A.M., Liskamp, R.M.J., Nijkamp, F.P.: Peptoid–peptide hybrids that bind syk SH2 domains involved in signal transduction. ChemBioChem. **2**, 171–179 (2001)
19. Seurynck-Servoss, S.L., Dohm, M.T., Barron, A.E.: Effects of Including an N-terminal insertion region and arginine-mimetic side chains in helical peptoid analogues of lung surfactant protein b. Biochemistry **45**, 11809–11818 (2006)
20. Miller, S.M., Simon, R.J., Ng, S., Zuckermann, R.N., Kerr, J.M., Moos, W.H.: Comparison of the proteolytic susceptibilities of homologous L-amino acid, D-amino acid, and N-substituted glycine peptide and peptoid oligomers. Drug Dev. Res. **35**, 20–32 (1995)
21. Miller, S.M., Simon, R.J., Ng, S., Zuckermann, R.N., Kerr, J.M., Moos, W.H.: Proteolytic studies of homologous peptide and N-substituted glycine peptoid oligomers. Bioorg. Med. Chem. Lett. **4**, 2657–262 (1994)
22. Lee, J., Udugamasooriya, D.G., Lim, H.-S., Kodadek, T.: Potent and selective photo-inactivation of proteins with peptoid-ruthenium conjugates. Nat. Chem. Biol. **6**, 258–260 (2010)
23. Fowler, S.A., Blackwell, H.E.: Structure–function relationships in peptoids: recent advances toward deciphering the structural requirements for biological function. Org. Biomol. Chem. **7**, 1508–1524 (2009)
24. Gorske, B.C., Nelson, R.C., Bowden, Z.S., Kufe, T.A., Childs, A.M.: "Bridged" n→π* interactions can stabilize peptoid helices. J. Org. Chem. **78**, 11172–11183 (2013)
25. Huang, M.L., Ehre, D., Jiang, Q., Hu, C., Kirshenbaum, K., Ward, M.D.: Biomimetic peptoid oligomers as dual-action antifreeze agents. Proc. Natl. Acad. Sci. U. S. A. **109**(19922–19927), S19922/1–S19922/20 (2012)
26. Ham, H.O., Park, S.H., Kurutz, J.W., Szleifer, I.G., Messersmith, P.B.: Antifouling glycocalyx-mimetic peptoids. J. Am. Chem. Soc. **135**, 13015–13022 (2013)
27. Olsen, C.A., Ziegler, H.L., Nielsen, H.M., Frimodt-Moeller, N., Jaroszewski, J.W., Franzyk, H.: Antimicrobial, hemolytic, and cytotoxic activities of β-peptoid-peptide hybrid oligomers: improved properties compared to natural AMPs. Chem. BioChem. **11**, 1356–1360 (2010)
28. Izzo, I., De Cola, C., De Riccardis, F.: Properties and bioactivities of peptoids tagged with heterocycles. Heterocycles **82**, 981–1006 (2011)
29. Lam, K.S., Lebl, M., Krchnak, V.: The "One-Bead-One-Compound" combinatorial library method. Chem. Rev. **97**, 411–448 (1997)
30. Ford, B.K., Hamza, M., Rabenstein, D.L.: Design, synthesis, and characterization of heparin-binding peptoids. Biochemistry **52**, 3773–3780 (2013)
31. Alluri, P.G., Reddy, M.M., Bachhawat-Sikder, K., Olivos, H.J., Kodadek, T.: Isolation of protein ligands from large peptoid libraries. J. Am. Chem. Soc. **125**, 13995–14004 (2003)
32. Liu, R., Lam, K.S.: Automatic Edman microsequencing of peptides containing multiple unnatural amino acids. Anal. Biochem. **295**, 9–16 (2001)
33. Udugamasooriya, D.G., Dineen, S.P., Brekken, R.A., Kodadek, T.: A peptoid "antibody surrogate" that antagonizes VEGF receptor 2 activity. J. Am. Chem. Soc. **130**, 5744–5752 (2008)
34. Aebersold, R., Mann, M.: Mass spectrometry-based proteomics. Nature **422**, 198–207 (2003)
35. Dodds, E.D.: Gas-phase dissociation of glycosylated peptide ions. Mass Spectrom. Rev. **31**, 666–682 (2012)
36. Konermann, L., Stocks, B.B., Pan, Y., Tong, X.: Mass spectrometry combined with oxidative labeling for exploring protein structure and folding. Mass Spectrom. Rev. **29**, 651–667 (2010)
37. Paizs, B., Suhai, S.: Fragmentation pathways of protonated peptides. Mass Spectrom. Rev. **24**, 508–548 (2005)
38. Gibson, C., Sulyok, G.A.G., Hahn, D., Goodman, S.L., Holzemann, G., Kessler, H.: Nonpeptidic alpha(v)beta(3) integrin antagonist libraries: on-bead screening and mass spectrometric identification without tagging. Angew. Chem. Int. Ed. **40**, 165–169 (2001)
39. Paulick, M.G., Hart, K.M., Brinner, K.M., Tjandra, M., Charych, D.H., Zuckermann, R.N.: Cleavable hydrophilic linker for one-bead-one-compound sequencing of oligomer libraries by tandem mass spectrometry. J. Comb. Chem. **8**, 417–426 (2006)
40. Thakkar, A., Cohen, A.S., Connolly, M.D., Zuckermann, R.N., Pei, D.: High-throughput sequencing of peptoids and peptide-peptoid hybrids by partial Edman degradation and mass spectrometry. J. Comb. Chem. **11**, 294–302 (2009)
41. Heerma, W., Boon, J.-P.J.L., Versluis, C., Kruijtzer, J.A.W., Hofmeyer, L.J.F., Liskamp, R.M.J.: Comparing mass spectrometric characteristics of peptides and peptoids. 2. J. Mass Spectrom. **32**, 697–704 (1997)
42. Heerma, W., Versluis, C., de Koster, C.G., Kruijtzer, J.A.W., Zigrovic, I., Liskamp, R.M.J.: Comparing mass spectrometric characteristics of peptides and peptoids. Rapid Commun. Mass Spectrom. **10**, 459–64 (1996)
43. Kruijtzer, J.A.W., Hofmeyer, L.J.F., Heerma, W., Versluis, C., Liskamp, R.M.J.: Solid-phase syntheses of peptoids using Fmoc-protected N-substituted glycines: the synthesis of (retro)peptoids of leu-enkephalin and Substance P. Chem. Eur. J. **4**, 1570–1580 (1998)
44. Ruijtenbeek, R., Versluis, C., Heck, A.J.R., Redegeld, F.A.M., Nijkamp, F.P., Liskamp, R.M.J.: Characterization of a phosphorylated peptide and peptoid and peptoid-peptide hybrids by mass spectrometry. J. Mass Spectrom. **37**, 47–55 (2002)
45. Sarma, B.K., Kodadek, T.: Submonomer synthesis of a hybrid peptoid-azapeptoid library. ACS Comb. Sci. **14**, 558–564 (2012)
46. Li, X., Guo, L., Casiano-Maldonado, M., Zhang, D., Wesdemiotis, C.: Top-down multidimensional mass spectrometry methods for synthetic polymer analysis. Macromolecules **44**, 4555–4564 (2011)
47. Morishetti, K.K., Russell, S.C., Zhao, X., Robinson, D.B., Ren, J.: Tandem mass spectrometry studies of protonated and alkali metalated peptoids: enhanced sequence coverage by metal cation addition. Int. J. Mass Spectrom. **308**, 98–108 (2011)
48. Bogdanov, B., Zhao, X., Robinson, D.B., Ren, J.: Electron capture dissociation studies of the fragmentation patterns of doubly protonated and mixed protonated-sodiated peptoids. J. Am. Soc. Mass Spectrom. **25**, 1202–1216 (2014)
49. Roepstorff, P., Fohlman, J.: Proposal for a common nomenclature for sequence ions in mass spectra of peptides. Biomed. Mass Spectrom. **11**, 601 (1984)
50. Vreven, T., Montgomery Jr., J.A., Peralta, J.E., Ogliaro, F., Bearpark, M., Heyd, J.J., Brothers, E., Kudin, K.N., Staroverov, V.N., Kobayashi, R., Normand, J., Raghavachari, K., Rendell, A., Burant, J.C., Iyengar, S.S., Tomasi, J., Cossi, M., Rega, N., Millam, J.M., Klene, M., Knox, J.E., Cross, J.B., Bakken, V., Adamo, C., Jaramillo, J., Gomperts, R., Stratmann, R.E., Yazyev, O., Austin, A.J., Cammi, R., Pomelli, C., Ochterski, J.W., Martin, R.L., Morokuma, K., Zakrzewski, V.G., Voth, G.A., Salvador, P., Dannenberg, J.J., Dapprich, S., Daniels, A.D., Farkas, Ö., Foresman, J.B., Ortiz, J.V., Cioslowski, J., Fox, D.J.: Gaussian 09. Gaussian, Inc, Wallingford (2009)
51. Sabareesh, V., Balaram, P.: Tandem electrospray mass spectrometric studies of proton and sodium ion adducts of neutral peptides with modified N- and C-termini: synthetic model peptides and microheterogeneous peptaibol antibiotics. Rapid Commun. Mass Spectrom. **21**, 3227 (2007) **[Erratum to document cited in CA144:391386]**
52. Bensadek, D., Monigatti, F., Steen, J.A.J., Steen, H.: Why b, y's? Sodiation-induced tryptic peptide-like fragmentation of non-tryptic peptides. Int. J. Mass Spectrom. **268**, 181–189 (2007)
53. Dongre, A.R., Jones, J.L., Somogyi, A., Wysocki, V.H.: Influence of peptide composition, gas-phase basicity, and chemical modification on fragmentation efficiency: evidence for the mobile proton model. J. Am. Chem. Soc. **118**, 8365–8374 (1996)
54. Tsaprailis, G., Nair, H., Somogyi, A., Wysocki, V.H., Zhong, W., Futrell, J.H., Summerfield, S.G., Gaskell, S.J.: Influence of secondary structure on

the fragmentation of protonated peptides. J. Am. Chem. Soc. **121**, 5142–5154 (1999)
55. Paizs, B., Suhai, S., Harrison, A.G.: Experimental and theoretical investigation of the main fragmentation pathways of protonated H-Gly-Gly-Sar-OH and H-Gly-Sar-Sar-OH. J. Am. Soc. Mass Spectrom. **14**, 1454–1469 (2003)
56. Bachor, R., Rudowska, M., Kluczyk, A., Stefanowicz, P., Szewczuk, Z.: Hydrogen-deuterium exchange of α-carbon protons and fragmentation pathways in N-methylated glycine and alanine-containing peptides derivatized by quaternary ammonium salts. J. Mass Spectrom. **49**, 529–536 (2014)
57. Rudowska, M., Wieczorek, R., Kluczyk, A., Stefanowicz, P., Szewczuk, Z.: Gas-phase fragmentation of oligoproline peptide ions lacking easily mobilizable protons. J. Am. Soc. Mass Spectrom. **24**, 846–856 (2013)